Vibrational study of phase transitions in (CH3)3NHNO3

M. Mylrajan and T. K. K. Srinivasan

Citation: The Journal of Chemical Physics **89**, 1634 (1988); doi: 10.1063/1.455160
View online: http://dx.doi.org/10.1063/1.455160
View Table of Contents: http://scitation.aip.org/content/aip/journal/jcp/89/3?ver=pdfcov
Published by the AIP Publishing

Vibrational study of phase transitions in $(CH_3)_3NHNO_3$

M. Mylrajan and T. K. K. Srinivasan[a)]
Regional Sophisticated Instrumentation Centre, Indian Institute of Technology, Madras 600 036 India

(Received 13 November 1987; accepted 14 April 1988)

$(CH_3)_3$ $NHNO_3$ belongs to the monoclinic system with space group $P2_1/c$ (C_{2h}^5) with four molecules per unit cell. Raman and infrared spectra (10–5000 cm^{-1}) of single crystals and polycrystalline samples of $(CH_3)_3$ $NHNO_3$ and of its *N*-deuterated derivative were investigated in the temperature range 90–415 K. Assignments of the measured frequencies to the internal vibrational modes were obtained. A systematic temperature dependent study of frequencies, bandwidths and integrated intensities was performed. The results indicate the existence of phase transitions at 359 and 407 K and both phase transitions show thermal hysteresis, characteristic of first order. In the high temperature phases II and I, the cations and anions achieve reorientational motion.

I. INTRODUCTION

Ammonium nitrate in the solid state is an ionic crystal consisting of tetrahedral NH_4^+ cations and planar NO_3^- anions. These ions are not only coupled by strong ionic interaction but also by hydrogen bonding. Ammonium nitrate forms several stable polymorphs[1,2] as the temperature is lowered from the melting point to 10 K. Among these, three high temperature phases are thermally disordered, each with a different degree of molecular rotation. Raman and infrared studies of the phase transitions have been carried out by many researchers[3–6] from the point of view of orientational order and the dynamics of the orientational states of the NH_4^+ and NO_3^- ions.

It is of interest to determine the type and temperature of phase transitions of compounds with cations of various geometries, since rotation of cations would involve two or more nonequivalent axes with considerably different moments of inertia. Further with increasing substitution of hydrogen by methyl groups, the space group requirements for cationic rotation increases simultaneously. In the series $[(CH_3)_n NH_{4-n}]NO_3$ $n = 1, 2, 3,$ and 4, the symmetry and the size of the cation is systematically changed with increasing n, while the size of the anion remains constant throughout.

Vibrational spectra and differential scanning calorimetric studies[7,8] of $CH_3NH_3NO_3$ (1MANO) in the temperature range 30–400 K showed the existence of three phases. A thermal hysteresis characteristic of first order was observed in the phase II–I transition. Raman and infrared spectral features indicate phase I to be a plastic phase in which cations and anions achieve isotropic reorientational motion. On the other hand vibrational spectra[9] of tetramethylammonium nitrate (4MANO) the extreme member of the series revealed two phase transitions (three phases) very close to room temperature. In contrast to this tri- and tetramethylammonium chlorides (3MACL and 4MACL) have been reported to exhibit one and four phase transitions, respectively.[10,11]

When the anion in 3MACL was replaced by ClO_4^- (3MAP) which is of tetrahedral symmetry, two phase transitions at 397 and 480 K were observed.[12–14] It is therefore desirable to establish the phase transitions in trimethylammonium nitrate (3MANO) compared to 3MACL and 3MAP. NMR and differential thermal analysis[15] (DTA) of 3MANO indicate phase transitions at 359 and 407 K. In this paper, Raman and infrared studies of phase transitions and assignments of vibrational modes are reported for the first time. In this part we would like to develop the results obtained so far in order to obtain some insight into the mechanisms of the phase transitions.

II. EXPERIMENTAL

3MANO was prepared by mixing equimolar quantities of trimethylamine with nitric acid and subsequent recrystallization from isopropyl alcohol. Single crystals of 3MANO were obtained by slow evaporation of its aqueous solution. *N*-deuterated 3MANO was prepared by repeatedly dissolving 3MANO in D_2O (99.4%) and subsequent evaporation. Infrared spectra were recorded on Perkin–Elmer 983 and Polytec FIR 30 spectrometers in the ranges 5000–300 and 300–10 cm^{-1}, respectively. Fluorolube and nujol mull techniques were used in the infrared region. A polyethylene pellet method was used in the far infrared region.

Raman spectra were measured on single crystals, polycrystalline powders, and aqueous solutions using a standard 90° configuration. The laser employed was a Spectra-Physics Model 165 argon ion laser operating at 200–300 mW power on the 5145 Å line. The scattered radiation was analyzed with a Cary 82 triple monochromator. Spectral slit widths in the range 1–3 cm^{-1} were used, depending on the sample employed. The frequencies obtained are correct within ± 1 cm^{-1}. Most of the spectra were recorded with a scanning speed of 30 cm^{-1} min^{-1}. An all glass conventional type liquid nitrogen container cell provided with a heating coil was used for temperature dependent Raman spectral studies. A Specac variable temperature cell was used in the infrared studies. Thermocouple readings and Stokes/anti-Stokes ratios were used to estimate the sample temperatures. Temperatures measured with the therocouple were within ± 1 K. A single crystal x-ray diffraction analysis was carried out on an Enraf-Nonius CAD-4 x-ray diffractometer with MoK_α radiation.

a) To whom correspondence should be addressed.

 0021-9606/88/151634-08$02.10

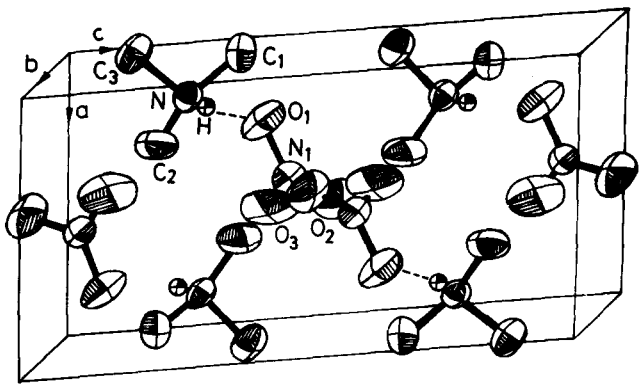

FIG. 1. Unit cell contents of 3MANO.

III. RESULTS AND DISCUSSION

A. Crystal structure

The crystal structure of 3MANO was solved by direct methods using the SHELX-76[16] program, based on 722 unique reflections (detailed analysis to be published separately). 3MANO belongs to the monoclinic system at 300 K with space group $P2_1/c$ (C_{2h}^5) containing four molecules per unit cell. The unit cell constants are: $a = 5.595(2)$; $b = 10.495(5)$; $c = 10.848(4)$ Å, and $\beta = 95.64(4)°$; $V = 633.9$ Å^3. Both cations and anions lie on general sites and are linked together by hydrogen bonds with N···O and O···H distances of 2.948 and 2.303 Å, respectively. The N–O distances for the NO_3^- ions are 1.240(5), 1.230(5), and 1.208(5) Å. The O–N–O angles are 119.6(4), 117.6(4), and 122.7(5)°. The N–C distances are 1.498(6), 1.500(7), and 1.483(7) Å. The C–N–C angles are 110.2(5), 112.0(5), and 110.7(5)°. Figure 1 represents the unit cell contents of 3MANO.

B. Vibrational spectra

The 36 vibrational degrees of freedom of the trimethylammonium ion under C_{3v} symmetry are distributed as $8A_1 + 4A_2 + 12E$ and the classification of the normal modes $\nu_1 - \nu_{24}$ to the different symmetry species are similar to those reported for 3MAX (X = Cl, Br, and I).[17] The internal modes of the cations and anions numbering 144 and 24, respectively, under the factor group C_{2h} are characterized as follows:

$$\Gamma \text{ internal } [(CH_3)_3NH^+]: \quad 36(A_g + B_g + A_u + B_u),$$

$$\Gamma \text{ internal } (NO_3^-): \quad 6(A_g + B_g + A_u + B_u).$$

The 45 external optical modes are represented as

$$\Gamma \text{ external: } 12(A_g + B_g) + 11A_u + 10B_u.$$

The gerade modes are Raman active and the ungerade modes are infrared active. The Raman tensor elements are aa, bb, cc, and ac for A_g and ab, bc for B_g. Figure 2 shows the single crystal Raman spectra of 3MANO at 300 K. The geometries used for single crystal Raman studies are $a(bb)c^*$ and $a(ba)c^*$, where a, b, and c^* form an orthogonal set.

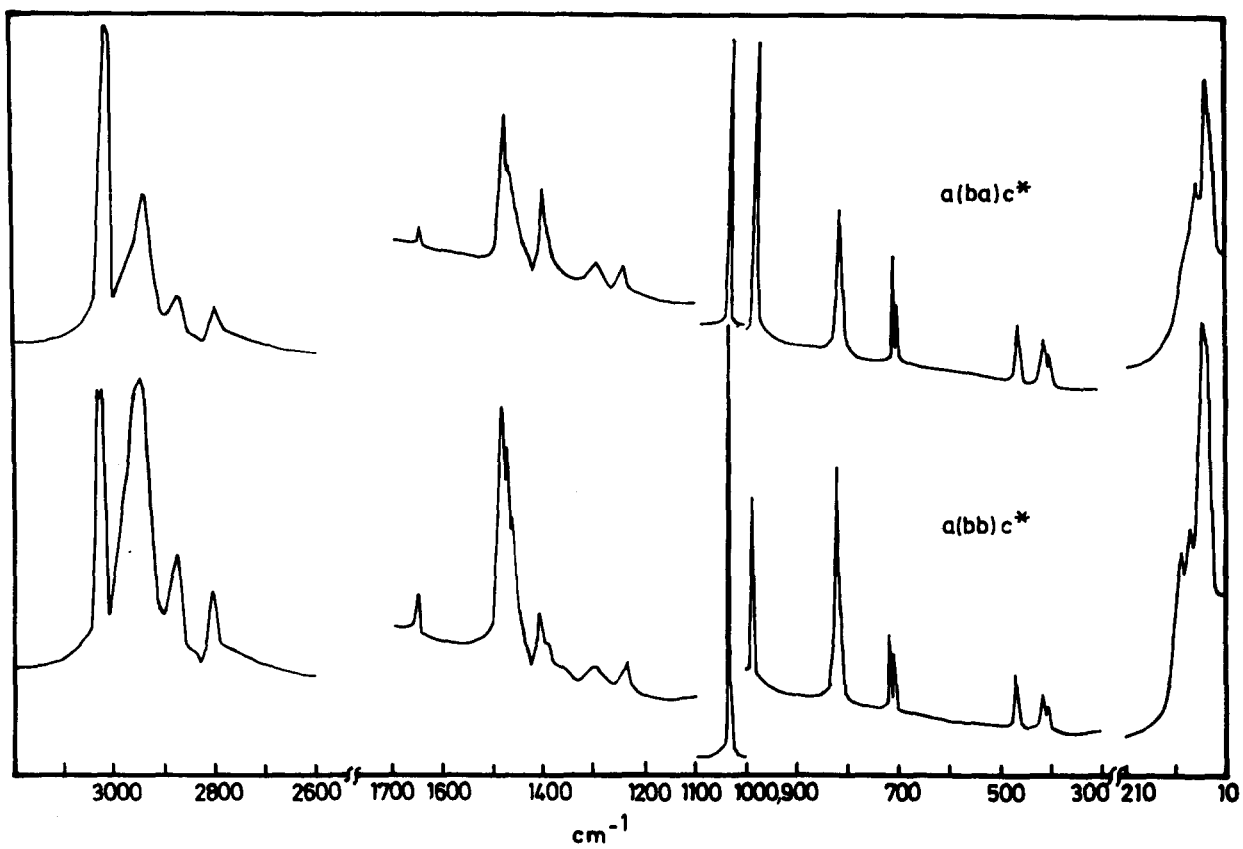

FIG. 2. Single crystal Raman spectra of 3MANO.

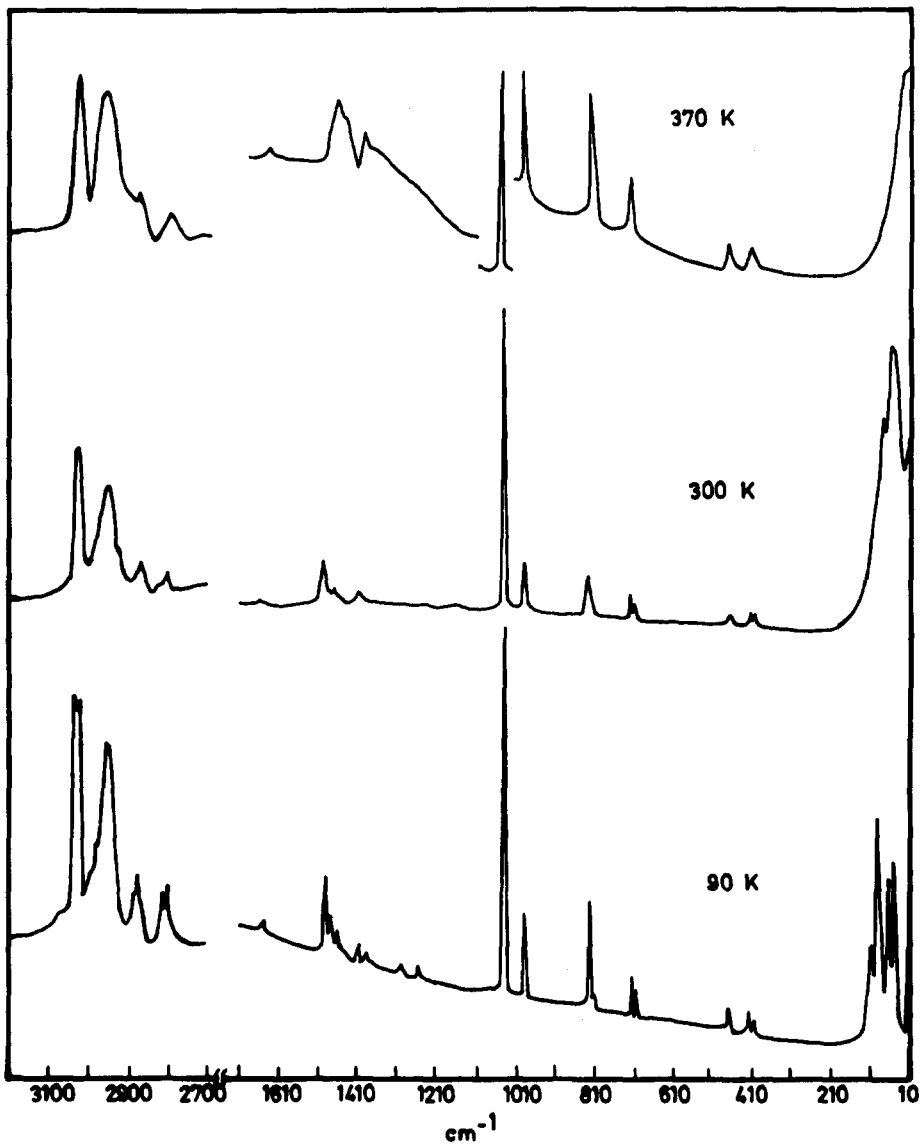

FIG. 3. Raman spectra of 3MANO (polycrystalline sample) at different temperatures.

Figures 3 and 4 represent the Raman and infrared spectra at different temperatures. Figure 5 represents the far infrared spectra at 300 and 90 K. The solid phases between 359 and 407 K, and above 407 K are referred to as phase II and I, respectively. Figure 6 represents the frequency variation of some of the infrared bands as a function of temperature. Since the sample showed signs of decomposition in the laser beam above 380 K, no Raman spectral measurements were taken in phase I. Peak positions and assignments are summarized in Table I. Symmetry classification of the normal modes of vibrations of the NO_3^- is as that of 1MANO.

Significant changes are observed in the Raman and infrared spectra of phase II compared to phase III. In the phase III–II transition, the ν_1' symmetric stretching mode shows a sudden shift in frequency at 359 K, with a concomitant increase in bandwidth and decrease in integrated intensity in the Raman and infrared spectra (Figs. 3 and 7, respectively). In the phase II–I transition, also the ν_1' infrared band shows an increase in integrated intensity and the $\gamma(CH_3)$ band shows decrease in frequency position with thermal hysteresis as shown in Fig. 8. The FWHM of the ν_2' infrared mode at 828 cm^{-1} shows a considerable increase in the phase III–II transition with thermal hysteresis as shown in Fig. 9. The ν_3' and ν_4' modes are degenerate. The bands due to ν_3' in the Raman spectrum of phase II are very weak and in phase III these are present at 1300 and 1385 cm^{-1}. In the infrared spectrum, strong bands due to the ν_3' mode are observed at 1305 and 1355 cm^{-1} in phase III and 1305 and 1358 cm^{-1} in phase II. In the Raman spectrum of phase III at 90 K for the ν_4' mode, site group splitting of the order of 11 cm^{-1} is observed while the splitting is reduced to 8 cm^{-1} in phase II.

The assignments of the normal modes of vibrations of the cations of 3MANO compare well with those of other trimethylammonium halides.[17] Both 3MANO and 3MACL belong to monoclinic systems but the site symmetry in the former is C_1, whereas it is C_s in the latter.

Both NC_3 and CH_3 group vibrations show considerable temperature dependence. The nondegenerate vibrations show a slight downward trend in the high temperature phase II. The NC_3 symmetric stretch at 820 cm^{-1} in the Raman

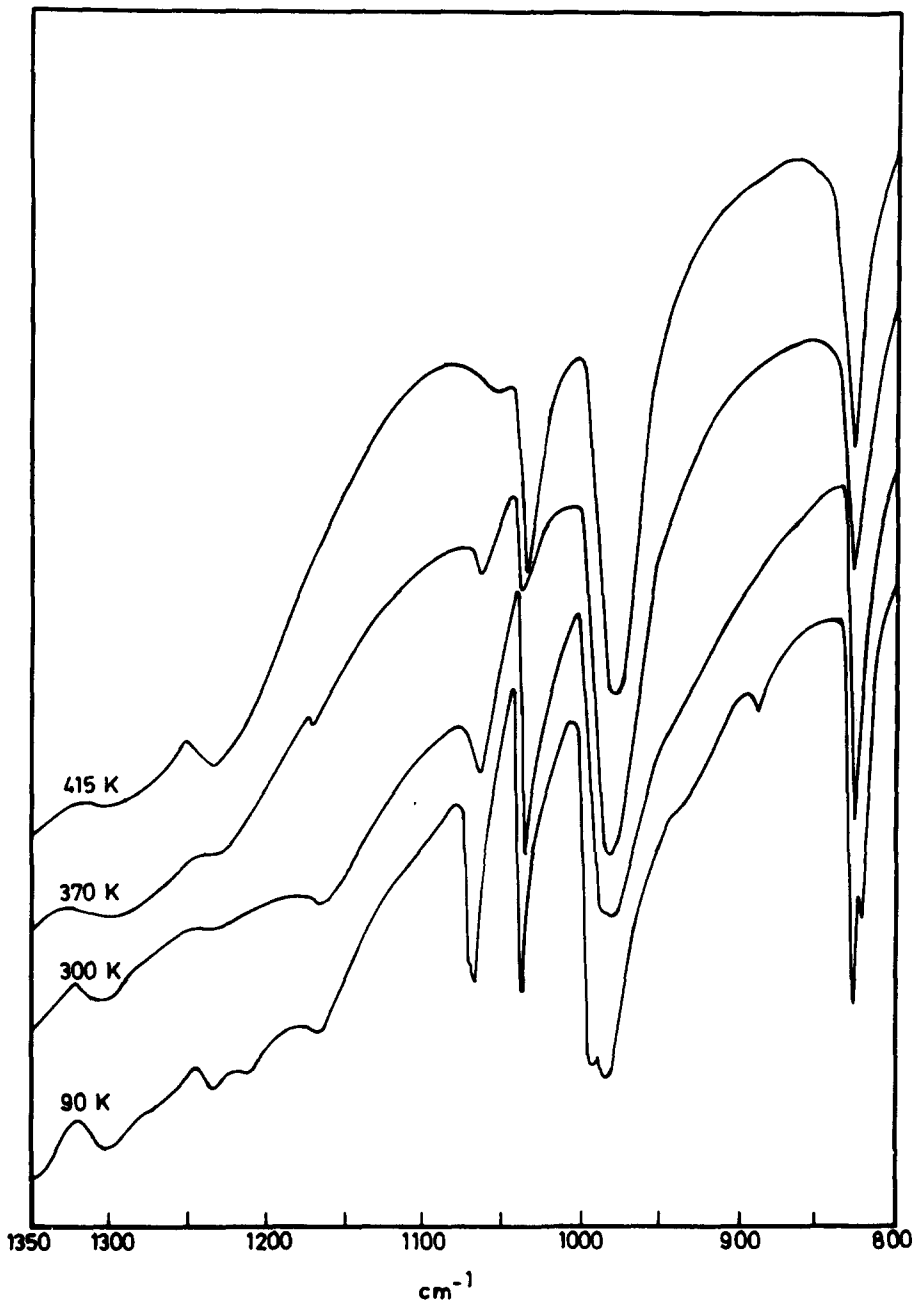

FIG. 4. Infrared spectra of 3MANO at different temperatures.

spectra of phase III shifts to 818 cm^{-1} in phase II, and the FWHM shows a sudden increase at the phase transition temperature. The NC_3 asymmetric stretch shows a single broad band at 986 cm^{-1} in the Raman spectrum of phase III, and at 90 K the site group splitting due to the removal of degeneracy is shown by the presence of two bands at 991 and 994 cm^{-1}. In the Raman spectrum of phase II only one band is observed at 984 cm^{-1}. The infrared spectrum also shows similar changes except that the splitting not observed in Raman spectra is present in phase III at 300 K.

For the deformation vibrations of the NC_3 group, a nondegenerate mode and a doubly degenerate mode are expected under the point group C_{3v}. Raman spectrum of phase III shows a doublet at 406 and 416 cm^{-1} similar to 3MAX (where X = Cl, Br, I, and ClO_4) consequent to the removal of degeneracy at the site C_1, whereas in phase II, a single weak and broad band at 415 cm^{-1} is observed. The CH_3 rocking mode at 1068 cm^{-1} in phase III in the infrared spectrum shows considerable temperature dependence. It appears as a doublet at 1071 and 1074 cm^{-1} at 90 K. In phase II it shifts to 1066 cm^{-1} and appears as a broad band. At the phase II–I transition, also, it shows a sudden shift in frequency with thermal hysteresis as shown in Fig. 8.

The part of the infrared spectrum near 3000 cm^{-1} is complex. The νNH in phase III appears at 3065 cm^{-1} at 300 K, while at 90 K it appears at 3070 cm^{-1} which shifts to 2290 cm^{-1} in the *N*-deuterated analog. The N–H···O distance 2.948 Å is comparable with 2.938 Å observed for 3MAP.[14] However the νNH of 3MAP at 3160 cm^{-1} is higher than that of 3MANO indicating that the hydrogen bond-

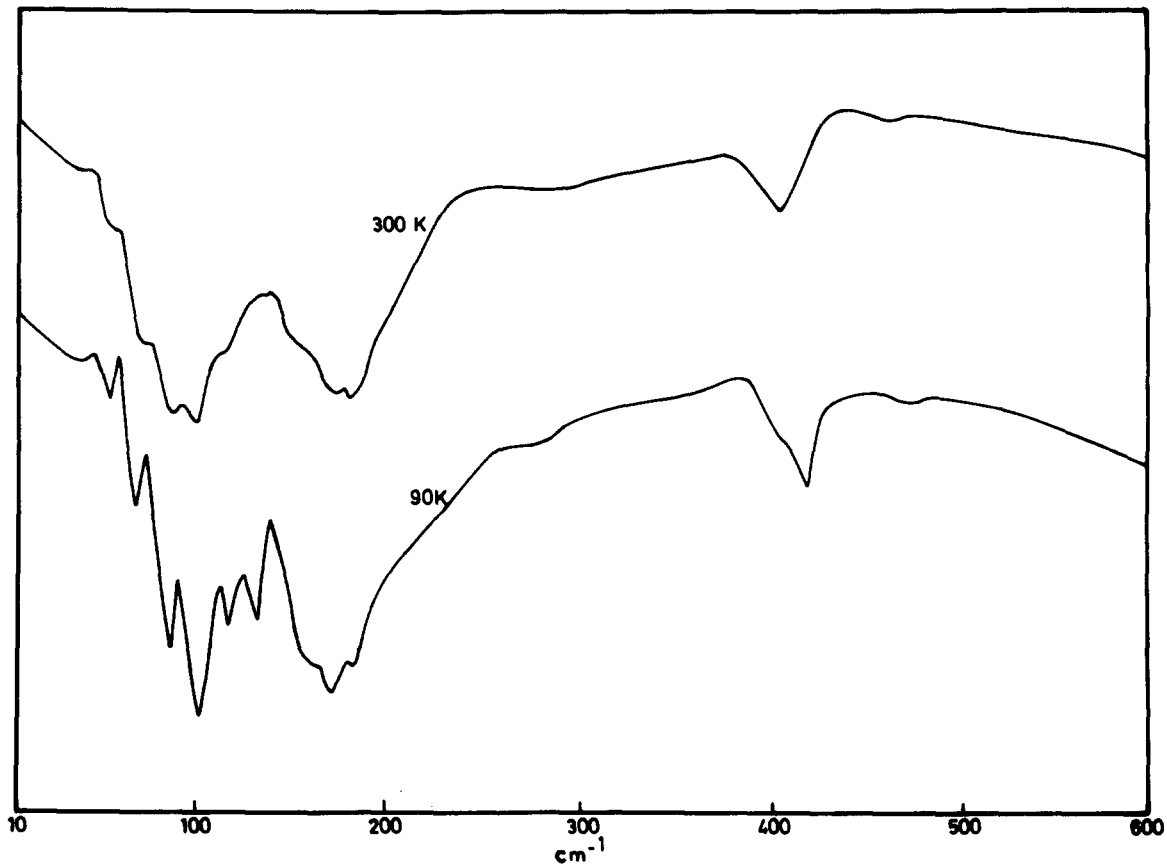

FIG. 5. Far infrared spectra of 3MANO at 300 and 90 K.

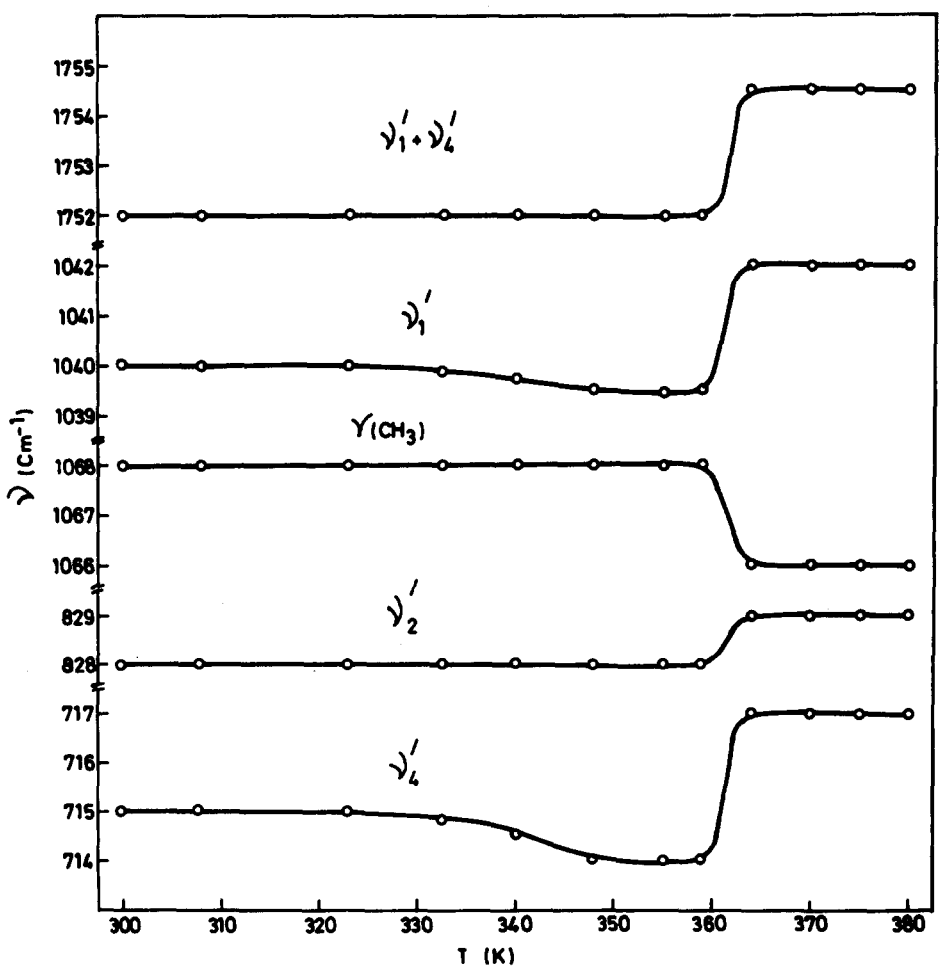

FIG. 6. Frequency variation of some infrared bands of 3MANO as a function of temperature in the phase III–II transition (temperature increasing).

TABLE I. Raman and infrared frequencies (cm^{-1}) and assignments for 3MANO.

Raman			Infrared				
Phase II	Phase III		Phase I	Phase II	Phase III		
370 K	300 K	90 K	412 K	370 K	300 K	90 K	Assignments
1	2	3	4	5	6	7	8
	45 A_g	49			44	45	
40	53 A_g	64			65	68	Translations
	55 B_g	70					and
	75 A_g, B_g	75			78	80	librations
	81 A_g	90			85	90	of cations
	95 A_g	101			98	100	and anions
	105 B_g	110			118	121	
						131	
					153	157	
					168	168	
					180	181	
					285	290	ν_{24}, τ CH_3
	406 A_g, B_g	409		408	408	407	ν_{23}, δCN
415	416 A_g, B_g	421	417	417	416	417	
	466 B_g						
467	468 A_g	473	466	466	468	468	ν_8, δCN
708	708 A_g, B_g	707		707	705	706	ν_4'
716	717 A_g, B_g	718	717	716	714	717	
	813 A_g	819					$2\nu_{23}$
818	820 A_g, B_g	824			822	824	ν_7, ν CN
			828	828	828	829	ν_2'
984	986 A_g, B_g	991	982	984	985	988	ν_{22}, ν CN
		994			992	995	
					1022	1024	ν_1' ($N^{18}O^{16}O_2^-$)
1041	1040 A_g, B_g	1043	1038	1042	1040	1040	ν_1'
		1049	1060	1066	1068	1071	
						1074	
1248	1248 A_g, B_g	1257	1235	1235	1238	1240	γ CH_3
					1253	1257	
			1295	1295	1295	1290	
1300	1300 A_g, B_g	1305	1305	1305	1305	1305	ν_3'
1385	1385 A_g	1385	1360	1358	1355	1370	
	1400 A_g	1394					ν_5, ν_{19}
1410	1410 A_g, B_g	1408	1408	1408	1408	1410	δCH_3 sym.
	1450 A_g, B_g	1450					
1466	1465 A_g, B_g	1465	1465	1465	1470	1465	ν_4, ν_{10}
1480	1476 A_g	1481	1478	1478	1480	1480	ν_{16}, ν_{17}
	1487 B_g	1493					δCH_3 asym.
	1488 A_g	1497					
1652	1653 A_g	1655					$2\nu_2'$
			1745	1745	1746	1744	$\nu_1' + \nu_4'$
				1755	1752	1754	
			2100	2100	2100	2100	
					2320	2320	Overtones and
			2420	2420	2420	2410	combinations
					2515	2515	of δCH_3, γ CH_3
					2545	2542	and δCN
			2735	2735	2730	2730	
2803	2804 A_g, B_g	2803	2800	2800	2800	2800	Combinations
	2813 A_g, B_g	2815					and overtones
			2845	2845	2850	2850	of δCH_3
2877	2878 A_g, B_g	2885					
2960	2954 A_g, B_g	2952	2950	2950	2950	2950	ν_2, ν_{15}; ν CH_3 sym.
		2959					
		2985					
		2995					
		3024					
	3027 A_g	3028					
3030	3034 B_g	3034	3035	3035	3035	3035	ν_1, ν_9, ν_{13}, ν_{14}
	3035 A_g	3037					ν CH_3 asym.
	3065 A_g	3070	3055	3055	3065	3070	ν_3, νNH
			4015	4015	4016	4020	ν CH_3 + γ CH_3
			4275	4275	4272	4275	ν CH_3 + ν CN
			4427	4427	4428	4430	
			4462	4462	4460	4465	ν CH_3 + δCH_3
			4500	4500	4500	4500	

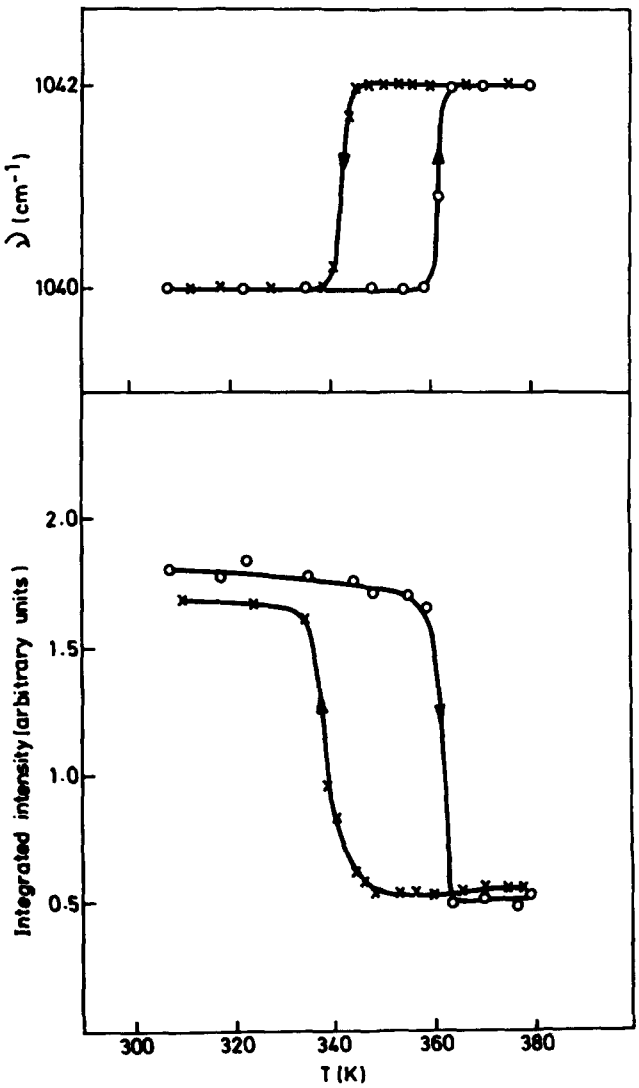

FIG. 7. Hysteresis in the frequency and integrated intensity variation of ν_1' infrared mode of 3MANO as function of temperature in phase III–II transition.

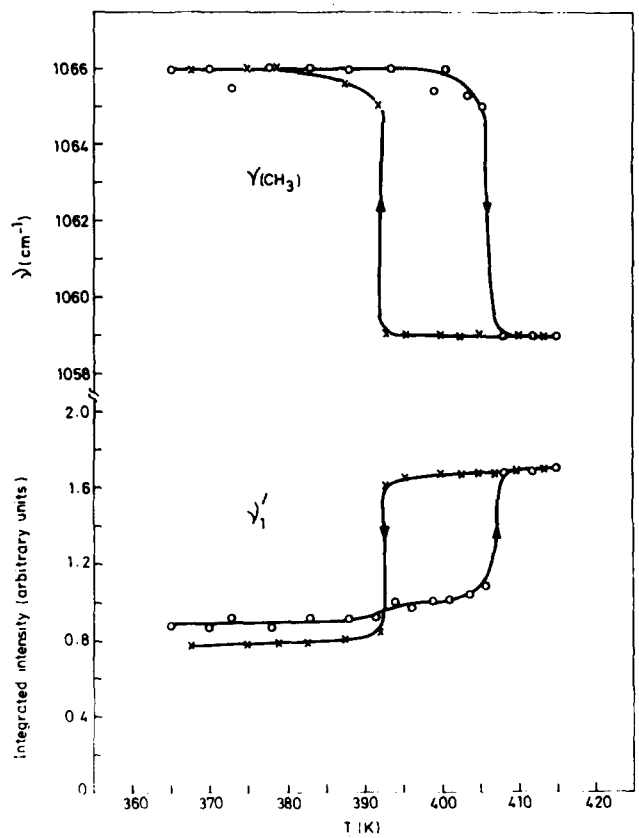

FIG. 8. Frequency variation of the CH_3 rocking mode and integrated intensity variation of the ν_1' mode of 3MANO in the infrared spectra as a function of temperature in phase II–I transition.

ing in 3MANO is stronger than that in 3MAP. It has been reported[18] that the νNH frequency of a salt of a complex tertiary amine varied from 2600 to 2800 to 3000 cm^{-1} as the anion to which the NH was hydrogen bonded changed from Cl^- to Br^- to ClO_4^-. The νNH of 3MANO is in accordance with the above specified range, as well as with the electronegativities of the anions involved in hydrogen bonding. In phase II and I, νNH appears as a broad band at 3055 cm^{-1} and merges with the C–H stretching vibrations. In the Raman spectrum νNH appears as a very weak band at 3065 cm^{-1} at 300 K.

The Raman spectrum in the lattice region is comprised of translational and librational modes of both cations and anions. These bands show a slight upward shift in band positions at 90 K, without any significant change in the number of bands. The upward shift at 90 K may be due to the lattice contraction. The spectra in phase II and above showed remarkable changes, in that only a shoulder on the Rayleigh wing at 40 cm^{-1} was observed.

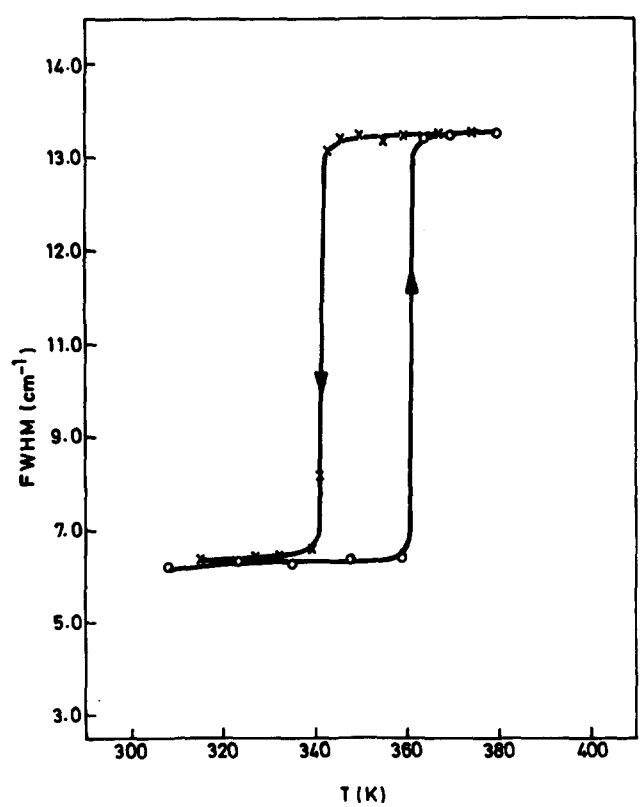

FIG. 9. Hysteresis of the FWHM (full width at half maximum) variation of ν_2' mode in the infrared spectra of 3MANO in phase III–II transition.

C. Phase transitions

The results clearly reveal that 3MANO undergoes phase transitions at 359 and 407 K. The sudden frequency shift and increase in FWHM for the ν_1' and CH_3 rocking vibrations (Figs. 7 and 8) followed by similar behavior of the ν_2' mode (Fig. 9) with thermal hysteresis in agreement with DTA results,[15] indicate that the phase III–II and II–I transitions are of first order, characterized by sudden changes in atomic rearrangements. The thermal hysteresis is about 20 K in the phase III–II transition, whereas it is about 14 K in the phase II–I transition. These values are comparable to that of 1MANO (20 K) in the phase II–I transition. The close similarity of the temperature dependent vibrational spectra in the internal mode region of the NO_3^- ion of 3MANO with those of 1MANO, show that the motional behavior of the NO_3^- in phase I appears to be similar in the two compounds. The broad and weak nature of the CH_3 rocking modes in phase II and I reveal CH_3 reorientations in both phases. NMR results[15] for 3MANO also support the present vibrational studies in the existence of three phases and the results showed that in phase II the cation exhibits reorientation about the C_3 axis and in phase I it exhibits rapid isotropic reorientation about its center of gravity and self-diffusion. The phase I is a plastic crystalline phase similar to phase I of 1MANO.

The advantage of the Raman technique is that group vibrations involving specific bonds give information about orientational motion. Considering the cation $(CH_3)_3NH^+$, the NC_3 and CH_3 vibrational bands in 3MANO will be affected by reorientational motions. As can be seen in Figs. 2 and 3 and Table I, while most of the degenerate modes of NC_3 show splitting in phase III, the removal of degeneracy appears complete at 90 K. In the absence of a phase transition, thermal treatment gives rise to progressive changes in frequency, band shape or intensity, while quite dramatic changes are often observed over relatively narrow temperature ranges due to a phase transition. The broad nature of the bands at 300 K compared to those at 90 K clearly indicate the effect due to thermal broadening, whereas the sudden significant changes occurring in the spectra (Figs. 6, 7, and 9) at 359 K cannot be attributed solely to thermal broadening and consequently the disappearance of the splitting in phase II is due to phase transition occuring at 359 K with thermal hysteresis. *N*-deuteration did not affect the phase transitions and similar results were obtained from DTA analysis.

Broadening and the absence of splitting observed in phase II and I indicate that degeneracy is restored. The crystal structures of 3MANO in phase II and I are not known. Hence it may be worthwhile to draw inference concerning the nature of phase I of 3MANO by comparing the spectra of 3MANO with that of the α phase of 3MACL since both of them have the same cation. 3MACL in α phase has been shown[10] to belong to the tetragonal system with disordered cations. Since the temperature dependence of the internal vibrations of the NC_3 group are very similar in these two compounds, it is possible that such a disorder, brought about by the reorientational motion of the NC_3 group around its threefold axis, is also present in phase II and I of 3MANO.

[1] C. Choi and H. J. Prask, Acta Cryst. B **39**, 414 (1983).
[2] M. Ahtee, K. J. Smolander, B. W. Lucas, and A. W. Hewat, Acta Cryst. **39**, 651 (1983).
[3] A. Theoret and C. Sandorfy, Can. J. Chem. **42**, 57 (1964).
[4] R. Newman and R. S. Halford, J. Chem. Phys. **18**, 1276 (1950).
[5] H. C. Tang and B. H. Torrie, J. Phys. Chem. Solids **38**, 125 (1977).
[6] K. Akiyama, Y. Morioka, and I. Nakagawa, Bull. Chem. Soc. Jpn. **54**, 1662 (1981).
[7] M. Mylrajan, T. K. K. Srinivasan, and G. Sreenivasamurthy, J. Cryst. Spectrosc. Res. **15**, 493 (1985).
[8] M. Mylrajan and T. K. K. Srinivasan, J. Raman Spectrosc. **16**, 412 (1985).
[9] M. Mylrajan and T. K. K. Srinivasan, J. Phys. C **21**, 1673 (1988).
[10] M. Stammler, J. Inorg. Nucl. Chem. **29**, 2203 (1967).
[11] M. Pal, G. S. Raghuvanshi, and H. D. Bist, Chem. Phys. Lett. **92**, 85 (1982).
[12] M. Stammler, R. Bruenner, W. Schmidt, and D. Orcutt, Adv. X-Ray Anal. **9**, 170 (1966).
[13] S. Jurga, Phys. Status Solidi A **81**, 77 (1984).
[14] M. Mylrajan and T. K. K. Srinivasan, Spectrochim. Acta (in press).
[15] H. Ishida, R. Ikeda, and D. Nakamura, Ber. Bunsenges. Phys. Chem. **90**, 598 (1986).
[16] G. M. Sheldrick, SHELX-76. Program for Crystal Structure Determination (University of Cambridge, England, 1976).
[17] M. Schlaak, M. Couzi, and P. V. Huong, Ber. Bunsenges. Phys. Chem. **80**, 881 (1976).
[18] E. A. V. Ebsworth and N. Sheppard, Spectrochim. Acta **13**, 261 (1959).